Published in final edited form as:
Dev Growth Differ. 2012 October ; 54(8): 739–752. doi:10.1111/dgd.12002.

Cartilage on the Move: Cartilage Lineage Tracing During Tadpole Metamorphosis

Ryan R. Kerney[1,2], **Alison L. Brittain**[3], **Brian K. Hall**[1], and **Daniel R. Buchholz**[3,*]

[1]Department of Biology, Dalhousie University, 1355 Oxford St., Halifax, NS B3H 4J1

[3]Department of Biological Sciences, University of Cincinnati, 312 Clifton Ct., Cincinnati, OH 45221

Abstract

The reorganization of cranial cartilages during tadpole metamorphosis is a set of complex processes. The fates of larval cartilage-forming cells (chondrocytes) and sources of adult chondrocytes are largely unknown. Individual larval cranial cartilages may either degenerate or remodel, while many adult cartilages appear to form de novo during metamorphosis. Determining the extent to which adult chondrocytes/cartilages are derived from larval chondrocytes during metamorphosis requires new techniques in chondrocyte lineage tracing. We have developed two transgenic systems to label cartilage cells throughout the body with fluorescent proteins. One system strongly labels early tadpole cartilages only. The other system inducibly labels forming cartilages at any developmental stage. We examined cartilages of the skull (viscero- and neurocranium), and identified larval cartilages that either resorb or remodel into adult cartilages. Our data show that the adult otic capsules, tecti anterius and posterius, hyale, and portions of Meckel's cartilage are derived from larval chondrocytes. Our data also suggest that most adult cartilages form de novo, though we cannot rule out the potential for extreme larval chondrocyte proliferation or de- and re-differentiation, which could dilute our fluorescent protein signal. The transgenic lineage tracing strategies developed here are the first examples of inducible, skeleton-specific, lineage tracing in *Xenopus*.

Keywords

Xenopus laevis; tadpole; metamorphosis; cartilage remodeling; chondrocyte lineage tracing; meganuclease transgenesis; Cre-recombinase; doxycycline; rtTA

Introduction

Cells that comprise post-metamorphic amphibian tissues can differentiate through one of two developmental pathways (Alberch, 1987; Alberch & Gale, 1986). In the "linear" pathway, adult tissues originate from differentiated cells that initially comprise larval tissues. The linear pathway may include de-differentiation of larval cells and re-differentiation into their adult versions (Alberch & Gale 1986) or the persistence of a single differentiated state. Alternatively, adult tissues may derive through a "compartmentalized"

*Corresponding Author: Department of Biological Sciences, University of Cincinnati, 312 Clifton Ct., Cincinnati, OH 45221, buchhodr@ucmail.uc.edu, phone: 513 556 9725, FAX: 513 556 5492.
[2]Currently: Department of Biology, Gettysburg College, 300 North Washington St., Gettysburg, PA 17325

Contributions:
RRK-Lab work, manuscript and figure preparation, ALB-data collection, BKH-manuscript preparation, DRB-Lab work, data collection, manuscript and figure preparation.

pathway, in which separate populations of stem or progenitor cells, which may be developmentally quiescent in the larvae, are induced to complete differentiation into adult tissues during metamorphosis. These pathways of differentiation have been investigated in multiple tissues and organs of metamorphosing frogs, through unique signatures of gene and protein expression, histomorphology, or markers of cell proliferation and death (e.g. Mukhi *et al.,* 2008; Nishikawa & Hayashi, 1999; Alley, 1989; Schreiber & Brown, 2003). These techniques can lead to results that are occasionally in conflict with one another (e.g., the intestinal epithelium: Schreiber *et al.,* 2005; Ishizuya-Oka *et al.,* 2003) and are arguably imprecise in identifying the larval origins of adult tissues. Thus, new methods are needed to elucidate pathways of differentiation in tadpole metamorphosis. This study aims to determine pathways of cellular differentiation (linear vs. compartmentalized) in the cartilaginous skull of metamorphosing *Xenopus laevis* tadpoles through novel transgenic cell-labeling techniques.

Compartmentalization of adult vs. larval cartilaginous skulls was first described for the paired adult epibranchial cartilages of the lungless salamander *Eurycea bislineata* (Smith, 1920; Alberch *et al.,* 1985; Alberch & Gale, 1986). Detailed anatomical studies revealed a larval perichondrial origin of the adult epibranchial cartilages, which superficially resembles the larval first epibranchial, although it is derived from a separate cell source. This initial observation of epibranchial compartmentalization was later extended to other plethodontid salamanders (Rose, 2009; Kerney *et al.,* 2012). However, no similar separate origins of adult cranial cartilages have been identified in other amphibian groups, including frogs (Hall, 2003). Begging the question: what is the extent of compartmentalization, if any, in the tadpole skull? The model frog *Xenopus laevis* is ideally suited for investigating cartilage compartmentalization given both their dramatic cranial metamorphosis (Trueb & Hanken, 1992) and the suite of molecular markers and tools available for developmental study (e.g., Chesneau *et al.,* 2008).

Our exploration of novel transgene labeling techniques began with the creation of separate inducer and reporter lines. The inducer line contains the chondrocyte-specific regulatory elements from the 5′ region and first intron of the *Xenopus tropicalis col2a1* gene (Kerney *et al.,* 2010). These activate the tetracycline/doxycycline conditional transcription factor rtTA, which in the presence of doxycycline (Dox), induces expression of Cre-recombinase (Cre) via the tetracycline/doxycycline response element (TRE) promoter in our transgenic line. The spatial expression of rtTA is restricted to cartilage by *col2a1* regulatory elements. Temporal control of TRE activation by rtTA depends on the addition of Dox to the rearing medium. This inducer line was crossed with one of two separate reporter lines.

Our first reporter line (Rankin *et al.,* 2009) has ubiquitous expression of cyan fluorescent protein (CFP) driven by the “constitutively active” cytomegalovirus (CMV) promoter. The CFP transgene sequence is flanked by loxP sites, followed by a red fluorescent transgene (DsRed2). CFP is excised by Cre and the flanking loxP sites are annealed, thereby shifting DsRed2 to be under control of the CMV promoter. When crossed with the Cre-expressing inducer line, dual transgenic inducer-reporter individuals (which we call the “Cre-dependent system”) have tissue-specific Cre expression that activates the expression of DsRed2 only in chondrocytes.

The second reporter line crossed with our inducer line does not use Cre to change fluorophore expression. Instead, these double transgenic tadpoles expressed GFP under the control of the TRE (tetracycline/doxycycline response element) promoter in the presence of rtTA and Dox (“rtTA-dependent system”). The rtTA-system allowed conditional labeling of tadpole chondrocytes using the cartilage-specific induction of GFP and lineage tracing of these chondrocytes through the persistence of GFP protein during metamorphosis. The rtTA

system was used to lineage trace the cartilaginous skull through both natural metamorphosis and triiodothyronine- (T3-) induced metamorphosis (e.g., Dodd & Dodd, 1976; Shi, 2000).

Materials and Methods

Plasmids and transgenesis

Standard restriction enzyme and PCR molecular cloning techniques were used to make the inducer construct pDPCol2.3rtTA-TRECre-HS4, where the *col2a1* regulatory sequences ("col2.3" sequence from Kerney *et al.,* 2010) replaced CMV, and Cre from pCSCRE2 (Ryffel *et al.,* 2003) replaced GFP in pDPCrtTA-TREG-HS4 (accn no. JF330265, Rankin *et al.,* 2009). Similarly, GFP replaced dpTR to make pDRTREG-HS4 from pDRTREdpTR-HS4 (accn no. JF330266, Rankin *et al.*, 2011). All portions of plasmids made using PCR were sequence verified. HS4 insulator elements were used to reduce chromosomal position effects on transgene expression (Allen & Weeks, 2005). These plasmids were used to make transgenic founders through the ISce-I meganuclease method of transgenesis (Thermes *et al.,* 2002; Ogino *et al.,* 2006a; Ogino *et al.,* 2006b; Pan *et al.,* 2006). Transgenic animals were detected by fluorescent protein in one or both eyes driven by the gamma-crystallin (CRY) promoter. Transgenic founders were reared to adulthood and checked for germ-line expression by breeding them with non-transgenic animals. All animal procedures were done in accordance with IACUC approval at the University of Cincinnati.

Doxycycline and thyroid hormone treatments

Tadpoles were treated with 50 μg/ml of doxycycline hyclate (Sigma). Treatment groups were either up to 30 Nieuwkoop-Faber stage (NF) 46 (Nieuwkoop & Faber, 1994) tadpoles in 30 mL, or up to 5 NF55–63 tadpoles in 200 mL. For the rtTA-dependent system, double transgenic tadpoles were treated for 2–3 days at odd-numbered stages from NF55–63. GFP fluorescence was observed just after Dox treatment and in subsequent odd-numbered stages through metamorphosis. Some NF46 tadpoles were also treated with 50 μg/mL Dox and/or 10 nM T3 (Sigma) to investigate cartilage lineage tracing during T3-induced metamorphosis. Treatments were carried out in the dark at room temperature with water and chemicals changed daily. Tadpoles were fed Sera Micron (Amazon.com) daily. However, no food was given to either the +T3 or −T3 control tadpoles in the induced metamorphosis experiments.

Transgene expression analysis

Fluorescent protein expression in live animals was observed using a Leica uorescence dissection microscope with CFP, GFP2, and RFP filter sets and photographed with a Leica DFC420 digital camera. Quantitative RT-PCR to measure GFP mRNA from hind limbs was carried out as previously described (Rankin *et al.,* 2009). Briefly, total RNA was extracted, contaminating genomic DNA removed, and cDNA made through reverse transcripiton. Quantitative PCR (QPCR) was carried out and analyzed using the delta Ct method (Livak & Schmittgen, 2001) for GFP (F-5′TGTCCACACAATCTGCCCTTTC, R-5′GCAGCTGTTACAAACTCAAGAAGGA, P-5′TTTCGTTGGGATCTTTC) and the housekeeping gene rpL8 (F-5′AGAAGGTCATCTCATCTGCAAACAG, R-5′CTTCAGGATGGGTTTGTCAATACGA, P-5′CAACCCCAACAATAGCT), using FAM-labeled TaqMan probes (Applied Biosystems). Three individuals per treatment group were used and significant differences between treatment groups with $p \leq 0.05$ were identified using ANOVA and Bonferroni post-hoc pairwise comparisons (JMP Statistical Software).

Results

Establishing Inducer and Reporter Lines

We transformed wild-type zygotes with the pDPcol2.3rtTA-TRECre-HS4 construct using meganuclease transgenesis (Fig. 1A). Of the 10 female and 13 male green-eyed transgenics reared to adulthood, only one female ("F10") and one male ("M4") passed the transgene when crossed to wild-type animals. The first reporter line pCLFR-SceI (used in our Cre-dependent system) was characterized previously (Rankin *et al.,* 2009). For the second reporter line pDRTREG-HS4 (used in our rtTA-dependent system), ten full transgenic founders from meganuclease injections were reared to adulthood and checked for germ-line transmission and GFP induction by crossing with the pDPcol2.3rtTA-TRECre-HS4 inducer line. Two males ("M2, M3") carried the transgene in their germ-line, with visually similar levels of Dox-inducible GFP in the F1 generation. One female was a germ-line carrier, but her offspring showed no GFP induction. The other seven were not germ-line carriers or were sterile after several breeding attempts. For the experiments described below, founders or F1 offspring of the pDPCol2.3rtTA-TRECre-HS4 lines were crossed with the established Cre-reporter transgenic line pCLFR-SceI (Rankin *et al.,* 2009) or with founders or F1 offspring of pDRTREG-HS4 lines.

Cre-dependent System: Cross pDPCol2.3rtTA-TRECre-HS4 with pCLFR-SceI

The inducer (pDPcol2.3rtTA-TRECre-HS4) and Cre-reporter (pCLFR-SceI) transgenic lines were designed to follow cartilage cell fate through metamorphosis through inducible and permanent transgene labeling (Fig. 1A, B). The cartilage-specific regulatory sequences from the 5′ region and first intron of the *Xenopus tropicalis col2a1* (Kerney *et al.,* 2010) in pDPcol2.3rtTA-TRECre-HS4 restrict expression of the transgenic transcription factor *rtTA* to chondrocytes. In the presence of doxycycline (Dox), rtTA protein activates the tetracycline/doxycycline-response element (TRE) of pDPcol2.3rtTA-TRECre-HS4 to drive *Cre* expression. Cre protein subsequently binds to the loxP sites on pCLFR-SceI to remove *CFP* and shift *DsRed2* under control of the ubiquitous cytomegalovirus promoter (CMV). Thus, upon treatment with Dox, all and only cartilage cells were expected to turn from blue to red.

Transgenic lines harboring the inducer construct (pDPCol2.3rtTA-TRECre-HS4) and the Cre-reporter (pCLFR-SceI) were crossed and the expected four types of progeny were obtained (Fig. 1C–E). Double transgenic tadpoles from pDPCol2.3rtTA-TRECre-HS4 x pCLFR-SceI were expected to have fluorescing blue bodies (from pCLFR-SceI), fluorescing green lenses (from pDPCol2.3rtTA-TRECre-HS4), and no red fluorescence in the absence of Dox treatment. Even though we found no leaky expression of DsRed2 from pCLFR-SceI single transgenic animals (Fig. 1E, third panel), red fluorescence was detectable in the absence of Dox induction in double transgenic tadpoles (Fig. 1E, fourth panel). Apparently, Cre was being expressed in cartilage cells to activate DsRed2 expression in the absence of Dox, likely due to *col2a1* regulatory elements activating Cre even when separated by the rtTA coding region (Suppl. Fig. 1A). Also, Dox did not have a positive affect on *col2a1* regulatory sequence activation of Cre, indicating that rtTA was not a significant factor for DsRed2 expression (Suppl. Fig. 1B). Thus, the "inducer" construct was effectively *col2a1*:Cre (i.e., constitutive Cre expression under control of the *col2a1* regulatory sequence with no influence from rtTA and TRE).

We reared double transgenic tadpoles and pCLFR-SceI single transgenic animals through metamorphosis. The CMV promoter of pCLFR-SceI is expected to give high levels of CFP expression all over the body at all stages. However, we found no CFP expression in tissues developing at NF53 or later (e.g., limb or girdle cartilages) and a gradual decrease in CFP

fluorescence intensity throughout the body as tadpoles grew (data not shown), suggesting that the CMV promoter stops initiating transcripts at some point between NF48–53. As a result, all larval cartilages present by NF50 are labeled with DsRed2, and cartilages arising at or after NF53 do not express DsRed2 due to lack of CMV activity in older tadpoles. Therefore, the Cre-dependent system enabled us to examine the fate of early-forming cartilages.

We examined double transgenic tadpoles at different stages before and during cranial remodeling (Fig. 2). DsRed2 expression in all larval cartilages was punctate (Fig. 2A, E), but intensified during metamorphic progression in the palatoquadrate and cranial trabeculae (Fig. 2B) and the ceratohyal/hyale (Fig. 2F, G, H). The increased intensity of DsRed2 expression in these cartilages may be attributable to compression as they remodel. In contrast, the metamorphosing Meckel's cartilages elongate down each side of the widening jaw. The punctate expression of DsRed2 in the larval lower jaw was still detectable, but became more dispersed as Meckel's cartilages elongated (Fig. 2H). Dorsal DsRed2 expression was still visible in the otic process of the palatoquadrate through NF63 (Fig. 2C) but was not visible by NF66 (Fig. 2D). For unknown reasons, some larval cartilages, such as the otic capsules and sub-ocular bar of the palatoquadrate, were not detectable with this system, and thus their fate could not be determined. Nevertheless, our results showed that the hyale and lower jaw of the adult are derived from the ceratohyal and Meckel's cartilages of the tadpole, respectively.

rtTA-dependent System: Cross pDPCol2.3rtTA-TRECre-HS4 with pDRTREG-HS4

Double transgenic animals from the cross pDPCol2.3rtTA-TRECre-HS4 x pDRTREG-HS4 gave the expected cartilage-specific, Dox-inducible, expression of GFP (Fig. 3). Only the double transgenic animals, as indicated by red and green fluorescence in the eyes, had Dox-dependent GFP expression in their cartilages. Lineage tracing in this transgenic system requires that production of GFP mRNA cease upon removal of Dox and the GFP protein remains detectable through metamorphosis. When NF46 tadpoles were treated with 50μg/mL Dox for two days, GFP intensity, though reduced, was still distinctly visible in larval cartilages at NF57–after 25 days and many-fold increases in size (data not shown). To determine whether the long-lasting GFP visibility was due to GFP protein stability or continued synthesis of GFP protein from mRNA, we compared GFP protein and mRNA expression in the hind limbs of NF57 tadpoles treated with Dox for three days then not treated for the following four days (Fig. 4). The hind limbs showed robust GFP fluorescence from Day 2 through Day 7 (Fig. 4A). GFP mRNA levels peaked by 2–3 days of Dox treatment, but quickly dropped to baseline levels after Day 5 (i.e., after two days without Dox; Fig. 4B). The long-lasting GFP protein stability and lack of GFP mRNA synthesis in the absence of Dox enabled use of this transgenic system to track the fate of larval cartilage cells through metamorphosis.

We examined cranial cartilages in detail here. The pectoral girdle and hind limbs are shown as supplemental figure (Fig. S2, S3), and other cartilages, such as the vertebral column, the forelimb, and the pelvic girdle had visible GFP but were not further examined. We found that the c*ol2a1* regulatory elements used in this study drive transcription in forming, rather than established, chondrocytes. This specificity can be seen by comparing images taken at NF59 of tadpoles treated with Dox at NF55–59 (Fig. 5A, C, E). Tadpoles are still increasing in size at NF55 and reach their maximum size at NF58. At NF59, larval dorsal cranial cartilages are labeled in animals induced with Dox at NF55 (Fig. 5A), less so at NF57 (Fig. 5C), and not at all when induced at NF59 (Fig. 5E), showing a correlation between GFP labeling intensity and cartilage growth.

Dorsal cranial cartilages—Larval dorsal cranial cartilages visible in these live transgenic tadpoles include the suprarostral plate, paired palatoquadrate, planum antorbital, tectum anterius, tectum posterius, and paired otic capsules. These cartilages are all labeled with GFP when double transgenics are treated with Dox at NF55 (Fig. 5A). However, only the otic capsule and tectum posterius at the back of the braincase clearly maintain GFP fluorescence during metamorphosis (NF63, Fig. 5B). The tectum anterius covers the posterior portion of each olfactory tract in tadpoles, and demarcates the anterior border of the frontoparietal fontanelle in adults (Trueb & Hanken, 1992). Faint paired cartilages corresponding to the paired tectum anterius carry GFP through NF63 following NF55 Dox induction (Fig. 5B). This cartilage lineage is even more pronounced following NF57 induction but is not discernable following NF59 induction (compare Fig. 5D and 5F). During NF57, a transient cartilaginous expansion of the planum antorbital is apparent (Fig. 5C) on the posterior border of the nasal capsules. This expansion of the planum antorbital does not correspond with an adult cartilage (Fig. 5D). Transient larval planum antorbital growth is also detectable in whole-mount clear-and-stained preparations, and this expanded anterior region is resorbed in NF59 tadpoles (R. Kerney personal observation). By NF59 and later stages, most larval dorsal cartilages are not labeled with GFP in the presence of Dox (Fig. 5E, F; data not shown). Tadpoles induced during NF59 show faint GFP expression in the otic capsules and none in the tectum posterius by NF63.

There is diffuse fluorescence on the dorsal braincase by NF63 following NF57 Dox induction, which does not topographically correspond to any cartilage, but may reveal a portion of the frontoparietal bone (see discussion).

Nasal capsule cartilages—The larval nares are largely unsupported by underlying cartilage, while the adult nares are encased in a nasal capsule that includes the nasal septum, alary, oblique and solum nasi cartilages. None of the adult nasal capsule cartilages carry detectable GFP protein from NF55 GFP-expressing chondrocytes (Fig. 5B). The alary cartilages become visible only in Dox-induced NF57 and later tadpoles and metamorphs (Fig. 5D–F). Similarly, the oblique cartilage is only visible in Dox-induced NF59 and later tadpoles and metamorphs (Fig. 5E, F; data not shown). The anterior-most edge of the nasal septum is labeled through NF57 Dox induction, while the entire element is labeled in NF59 (Fig. 5D–F). The solum nasi is an interior cartilage and is not visible in our material.

Ventral cranial cartilages—Ventral larval cranial cartilages visible in these live transgenic tadpoles include Meckel's, ceratohyal, and ceratobranchial cartilages. Similar to the larval dorsal cartilages, labeling of the ventral cartilages becomes increasingly less visible in Dox-induced tadpoles from NF55–59 (Fig. 6). Ceratobranchial labeling is not detectable in NF63 animals that are Dox-induced during NF55 and NF57 (Fig. 6C–F). In Dox-induced NF55 tadpoles, the ceratohyal remodels into the hyale while retaining the early GFP label (Fig. 6A, B; data not shown), as seen in the Cre-dependent system (Fig. 2). Meckel's cartilage labeled at NF55 is no longer detectable at NF63 using the rtTA-dependent system. Meckel's cartilage is never visible in Dox-induced NF57 tadpoles. Meckel's cartilage is faintly marked in its posterior and antero-medial ends in Dox-induced NF59 tadpoles, which can be seen in a remodeled location at NF63 (Fig. 6E, F).

rtTA-dependent System: Induced metamorphosis

This experiment tracked the fate of larval cartilages using induced metamorphosis to compare with the natural metamorphosis experiments described above. Two days of Dox treatment, inducing cartilage-specific GFP expression at NF46, preceded seven days of T3 treatment to induce metamorphic remodeling in double transgenic tadpoles (Fig. 7). All larval cartilages were labeled throughout each element following Dox treatment. By the end

of seven days of T3 treatment, complete larval cartilage resorption occurred in all but three elements which retained GFP labeling, namely the otic capsules, ceratohyal, and Meckel's cartilages. The latter two remodeled to form the hyale and lower jaw, respectively. Faint expression in the degrading ceratobranchials also persisted, although these cartilages would eventually resorb if followed for a longer duration. To identify new cartilage formation during induced metamorphosis, double transgenic tadpoles were treated with T3 for 7 days at NF46, with Dox induction beginning on Day 3, and imaged on Day 7 (Fig. 8). The nasal capsule cartilages, cartilages of the lower jaw (the antero-medial end of Meckel's cartilage), and the hyale had strong GFP labeling with this treatment protocol. GFP labeling of both the hyale and most of Meckel's cartilage was punctate.

Discussion

The complexity of cartilage remodeling makes the task of following the fate of tadpole cartilages challenging. The limitations of previous histological methods left many questions about the remodeling process unanswered. Using our transgenesis systems, we were able to mark chondrocytes and monitor their fate throughout the body in live tadpoles undergoing metamorphosis, giving a more precise characterization of the fate of tadpole cartilages.

Our two transgenic systems give complementary and overlapping information about the fate of larval cartilages (Table 1). In the Cre-dependent system (Figs. 1, 2), cartilage cells that form before metamorphosis are labeled with DsRed2. Cartilage-specific Cre-mediated DsRed2 expression is maintained by the CMV promoter until the CMV promoter becomes transcriptionally inactive sometime between NF48–53. After NF53, the DsRed2 protein persists, revealing the fate of early forming larval cartilages through metamorphosis. In the rtTA-dependent system (Figs. 3–8), growing cartilage at any stage can be inducibly labeled with GFP. The longevity of the GFP protein allows the persistence of cartilage labeling through metamorphosis.

We cannot rule out the possibility that larval chondrocytes de-differentiate, divide rapidly diluting out the GFP signal, then re-differentiate to form adult cartilages in either system. Though both systems are potentially subject to these false negatives, our GFP mRNA and protein analyses (Fig. 4) indicate that there are no false positives, such that adult cartilages carrying the larval GFP label are derived from differentiated tadpole chondrocytes.

Thus, we have definitively shown a linear pathway of differentiation for the larval otic capsule, tecti anterius ans posterius, ceratohyal, and Meckel's cartilage, as chondrocytes from these elements contribute to the adult versions of these elements. Our data also suggest compartmentalization of cells giving rise to chondrocytes of the nasal capsule and the ends of Meckel's cartilage, as these cartilages lack GFP labeling and thus do not appear to be derived from larval chondrocytes. Below, we discuss how results from these two systems support and extend previous research on cartilage development through metamorphosis.

Dorsal cranial cartilages

The otic capsules are connected by the dorsomedial tectum posterius. Both carried the GFP label in the rtTA-dependent system animals treated with Dox at NF55 (Fig. 5). Strong maintenance of premetamorphic labeling in the otic capsule in the rtTA-dependent system, and the near complete lack of labeling through later Dox induction (Figs. 5, 7), indicate the adult otic capsule is derived from the larval version. The anterior prootic and posterior exoccipital bones invest the adult otic capsule cartilage. These bones gradually replace most of the cartilage with the exception of the anterolateral crista prootica, which persists as a narrow band of cartilage in adults (Trueb & Hanken, 1992).

Recent fate mapping revealed the adult otic capsule to be derived from branchial arch neural crest (Gross & Hanken, 2008). However, earlier studies did not find crest contributions to the larval otic capsule or tectum posterius (Olsson & Hanken, 1996), suggesting that the larval otic capsule is derived from paraxial (somitic) mesoderm (see also Smit, 1953). The persistence of otic capsule labeling in the CRE-dependent system suggests that the adult otic capsule is derived from the same cells as the larval cartilage. These results, and the observations of Gross and Hanken (2008), controversially suggest a branchial arch neural crest origin for both the larval and adult otic capsule in frogs, which differs from the experimentally verified mesodermal origin of the salamander otic capsule (Piekarski & Olsson, 2007; Toerien, 1963).

The larval dorsal cranial cartilages that resorb during the stages observed in our material include the planum antorbital, suprarostral plate, and palatoquadrate. These were well labeled in tadpoles, and no longer visible after natural (Figs. 2 and 5) or T3-induced (Fig. 7) metamorphosis. During metamorphosis the palatoquadrate breaks several larval processes that connect it to the neurocranium, and establishes the adult pterygoid process while accommodating elongation of the lower jaw (Pusey, 1938; Wassersug & Hoff, 1979; Rose, 2009). The pterygoid bone covers most of the adult palatoquadrate. However, this extensive cartilage has a posterior maxillary process and ventrolateral process in the adult. Neither process is invested by bone, and both should be detectable through fluorescence imaging. It is surprising that adult palatoquadrate cartilages did not carry detectable fluorophores (NF 66; Fig. 2), because unlike other cartilages found in both the tadpole and adult, e.g., otic capsule and lower jaw, apparently no larval chondrocytes contribute to the adult palatoquadrate. This is particularly surprising since recent fate-mapping studies have shown both the larval and adult versions of the palatoquadrate are derived from branchial-arch neural crest cells (Gross & Hanken, 2008). Our data indicate that this common embryonic cell source is divided into progenitor cells contributing to the tadpole and adult versions of this apparently single cartilage.

Our results also suggest that cartilages of the adult nasal capsule are not derived from larval chondrocytes. The alary, oblique, and nasal septum cartilages are visible in the rtTA- but not CRE-dependent system. The lack of labeling in these nasal cartilages in the CRE-dependent system is consistent with the extinction of CMV promoter activity in later tadpole stages (described above). In the rtTA-dependent system, the alary and anterior nasal septum cartilages are first labeled during NF57, but the oblique cartilages are not detectable until NF59 (Fig. 5). Nasal cartilages are not observed during metamorphosis when GFP labeling is induced at NF55 (Figs. 5, 7). A non-chondrocyte larval origin of adult nasal capsule cartilages is in keeping with earlier descriptions of nasal capsule development and fate mapping in *Xenopus*. The origin of the adult nasal capsule cartilages is complex; cartilages are derived from the hyoid and mandibular stream neural crest as well as possible contributions from non-neural crest embryonic sources (Gross & Hanken, 2008). Studies from other frog families (outside the *Xenopus* family Pipidae) also reveal de novo formation of most nasal capsule cartilages with the exception of the solum nasi, which are continuous with the larval cornu trabeculae in the genus *Spea* (Pugener & Maglia, 2007). Pipids lack distinct cornu trabeculae. Instead they have a suparostral plate, which is of arguable homology to the cornu trabeculae of other tadpoles (see Kerney *et al.,* 2007). Morphological studies show that the fused suprarostral plate in Pipids does not remodel into any portion of their nasal capsule (Roček & Vesely, 1989). However, this could not be verified in our material since the solum nasi forms the floor of the adult nasal capsule, and was not discernable in any of our live transgenic froglets.

Ventral cranial cartilages

Results from both transgenic systems reveal the hyale as clearly derived from tadpole chondrocytes of the larval ceratohyal, while the ceratobranchials resorb. Hyale labeling is strong in the Cre- (Fig. 2H) but not rtTA-dependent system through natural metamorphosis (Fig. 6B), likely because only a fraction of the larval ceratohyal can be labeled during any one 2–3 day Dox treatment (Fig. 6A). However, larval ceratohyal labeling in the rtTA-dependent system is strong in early stages, and can be traced to the hyale in T3-induced metamorphosis (Fig. 7, bottom right panel).

Meckel's cartilage remodeling appears to be composed of both repositioned larval cartilages along its paired central shaft (Thompson, 1987), and production of new cartilage on its paired anteromedial and posterodistal ends. Our "natural metamorphosis" results reveal new cartilage on the paired proximal and distal ends of Meckel's cartilage that are derived from a non-chondrocyte source in the tadpole (Fig. 6F). Recent fate mapping research shows the posterodistal end of Meckel's cartilage is derived from a combination of hyoid and mandibular stream crest (Gross & Hanken, 2008), while the rest of the adult cartilage, and all of the larval cartilage, is derived from the mandibular arch neural crest (Sadaghiani & Thiébaud 1987; Olsson & Hanken, 1996; Gross & Hanken, 2008).

Dermal bone

There is faint green fluorescence corresponding to the frontoparietal bones at NF63 in the rtTA-dependent system, after induction at NF57 and NF59 with Dox, but not in those induced at NF55. These dermal bones of the skull vault are not prefigured in cartilage. Recent studies have shown a *col2a1*-expressing lineage of cells in mouse dermal bones of the skull vault and lower jaw (Ahberg *et al.,* 2005; Abzhanov *et al.,* 2007). Mouse *col2a1* expression in dermal bone is co-localized or preceded by several additional chondrocyte markers. However, this restricted chondrocyte-like cell lineage eventually become osteoblasts of the mature dermal bone. Our results are consistent with chondrocyte-like cells prefiguring the skull vault in anurans as well.

Unlike the faint expression in the frontoparietal in our material, GFP fluorescence is not apparent in other dermal bones of the upper jaw or face. This may be attributable to the position and thin layers of integument above the frontoparietal, while other dermal bones are less readily viewed through live imaging. Alternatively, chondrocyte-like precursor cells (or *col2a1* reporter expression in these cells) may not consistently occur in all dermal bones.

Conclusion

The Cre-dependent system (transient labeling of early cartilage elements) and the rtTA-dependent system (inducible labeling of new cartilage growth) are the first examples of inducible, skeleton-specific, transgene activation and subsequent lineage tracing in amphibians. The rtTA-dependent transgenic labeling approach represents a general method to mark cells for lineage tracing in a tissue-specific and inducible manner, which will be applicable to other tissues of interest by replacing the *col2a1* regulatory elements with tissue-specific promoters.

Using these novel dual transgenic lines, we show that pathways of cartilage differentiation vary in different regions of the tadpole skull. Several adult-specific cartilages, e.g., the nasal capsules, do not carry larval chondrocyte GFP labeling and thus appear to have a compartmentalized mode of differentiation. Tadpole-specific cartilages, e.g., ceratobranchials and planum antorbital, resorb without apparently contributing labeled chondrocytes to the adult. Finally, several cartilages are found in both tadpoles and adults, e.g., the otic capsules, lower jaw, and palatoquadrate. However the adult versions of these

cartilages are not necessarily derived from their larval counterparts. Chondrocytes of the larval otic capsule, ceratohyal, and lower jaw contribute to their adult counterparts, but apparently those of the larval palatoquadrate do not. The adult version of the palatoquadrate is apparently derived from a different cell population than its larval counterpart.

Our results beg the immediate question: where are the larval progenitor cells that give rise to adult cartilages in the skull? To date, we are unaware of research that conclusively identifies these cartilage progenitor cells in metamorphosing frogs, despite an extensive history of detailed anatomical research on anuran cranial metamorphosis. Continued exploration of novel transgene reporters may eventually help locate these progenitor cell populations, and provide insight into the uniquely dynamic cartilage development of metamorphosing frogs.

Supplementary Material

Refer to Web version on PubMed Central for supplementary material.

Acknowledgments

This work was supported by NIH R03 5F32DK010069-03 and NSF IOS 0950538 to D.R.B., an NSERC research grant to B. K. H., and an American Association of Anatomists Postdoctoral Fellowship to R.K.

References

Aberg T, Rice R, Rice D, Thesleff I, Waltimo-Siren J. Chondrogenic potential of mouse calvarial mesenchyme. J Histochem Cytochem. 2005; 53:653–663. [PubMed: 15872058]

Abzhanov A, Rodda SJ, Mcmahon AP, Tabin CJ. Regulation of skeletogenic differentiation in cranial dermal bone. Development. 2007; 134:3133–3144. [PubMed: 17670790]

Alberch, P. Evolution of a developmental process: irreversibility and redundancy in amphibian metamorphosis. In: Raff, R.; Raff, E., editors. Development as an Evolutionary Process. Alan R. Liss Inc; New York: 1987. p. 23-46.

Alberch P, Gale E. Pathways of cytodifferentiation during the metamorphosis of the epibranchial cartilage in the salamander *Eurycea bislineata*. Dev Biol. 1986; 117:233–244.

Alberch P, Lewbart G, Gale E. The fate of larval chondrocytes during the metamorphosis of the epibranchial in the salamander, *Eurycea bislineata*. J Embryol Exp Morphol. 1985; 88:71–83. [PubMed: 4078541]

Allen BG, Weeks DL. Transgenic *Xenopus laevis* embryos can be generated using phiC31 integrase. Nat Methods. 2005; 2:975–979. [PubMed: 16299484]

Alley K. Myofiber turnover is used to retrofit frog jaw muslces during metamorphosis. Am J Anat. 1989; 184:1–12. [PubMed: 2783829]

Chesneau A, Sachs LM, Chai N, et al. Transgenesis procedures in Xenopus. Biol Cell. 2008; 100:503–521. [PubMed: 18699776]

Dodd, M.; Dodd, J. The Biology of Metamorphosis. In: Lofts, B., editor. Physiology of the Amphibia. Vol. 3. Academic Press; New York: 1976. p. 467-599.

Gross J, Hanken J. Segmentation of the vertebrate skull: neural-crest derivation of adult cartilages in the clawed frog, *Xenopus laevis*. Int Comp Biol. 2008; 48:681–696.

Hall, BK. Developmental and cellular origins of the amphibian skeleton. In: Heatwole, H.; Davies, M., editors. Amphibian Biology, Volume 5: Osteology. Vol. 5. Surrey Beatty and Sons, Chipping Norton; Australia: 2003. p. 1551-1597.

Ishizuya-Oka A, Shimizu K, Sakakibara S, Okano H, Ueda S. Thyroid hormone-upregulated expression of Musashi-1 is specific for progenitor cells of the adult epithelium during amphibian gastrointestinal remodeling. J Cell Sci. 2003; 116:3157–3164. [PubMed: 12799417]

Kerney R, Gross JB, Hanken J. Runx2 is essential for larval hyobranchial cartilage formation in *Xenopus laevis*. Dev Dyn. 2007; 236:1650–1662. [PubMed: 17474117]

Kerney R, Hall BK, Hanken J. Regulatory elements of *Xenopus col2a1* drive cartilaginous gene expression in transgenic frogs. Int J Dev Biol. 2010; 54:141–150. [PubMed: 19757383]

Kerney RR, Blackburn DC, Muller H, Hanken J. Do larval traits re-evolve? Evidence from the embryogenesis of a direct-developing salamander, *Plethodon cinereus*. Evolution. 2012; 66:252–262. [PubMed: 22220879]

Nieuwkoop, PD.; Faber, J. Normal table of Xenopus laevis (Daudin). Garland Publishing; New York, London: 1994.

Mukhi S, Mao J, Brown DD. Remodeling the exocrine pancreas at metamorphosis in *Xenopus laevis*. Proc Natl Acad Sci U S A. 2008; 105:8962–8967. [PubMed: 18574144]

Nishikawa A, Hayashi H. T3-hydrocortisone synergism on adult-type erythroblast proliferation and T3-mediated apoptosis of larval-type erythroblasts during erythropoietic conversion in *Xenopus laevis*. Histochem Cell Biol. 1999; 111:325–334. [PubMed: 10219633]

Ogino H, Mcconnell WB, Grainger RM. High-throughput transgenesis in *Xenopus* using I-SceI meganuclease. Nat Protoc. 2006a; 1:1703–1710. [PubMed: 17487153]

Ogino H, Mcconnell WB, Grainger RM. Highly efficient transgenesis in *Xenopus tropicalis* using I-SceI meganuclease. Mech Dev. 2006b; 123:103–113. [PubMed: 16413175]

Olsson L, Hanken J. Cranial neural-crest migration and chondrogenic fate in the Oriental fire-bellied toad *Bombina orientalis*: defining the ancestral pattern of head development in anuran amphibians. J Morphol. 1996; 229:105–120.

Pan FC, Chen Y, Loeber J, Henningfeld K, Pieler T. I-SceI meganuclease-mediated transgenesis in *Xenopus*. Dev Dyn. 2006; 235:247–252. [PubMed: 16258935]

Piekarski N, Olsson L. Muscular derivative of the cranialmost somites revealed by long-term fate mapping in the Mexican axolotl (*Ambystoma mexicanum*). Evol Dev. 2007; 9:566–578. [PubMed: 17976053]

Pugener LA, Maglia AM. Skeletal morphology and development of the olfactory region of *Spea* (Anura: Scaphiopodidae). J Anat. 2007; 211:754–768. [PubMed: 18045351]

Pusey H. Structural changes to the anuran mandibular arch during metamorphosis, with reference to *Rana temporaria*. Q J Microsc Sci. 1938; 80:479–552.

Rankin SA, Hasebe T, Zorn AM, Buchholz DR. Improved cre reporter transgenic *Xenopus*. Dev Dyn. 2009; 238:2401–2408. [PubMed: 19653309]

Roček Z, Vesely M. Development of the ethmoidal structures of the endocranium in the anuran *Pipa pipa*. J Morphol. 1989; 200:301–309.

Rose CS. Generating, growing and transforming skeletal shape: insights from amphibian pharyngeal arch cartilages. Bioessays. 2009; 31:287–299. [PubMed: 19260024]

Ryffel GU, Werdien D, Turan G, Gerhards A, Goosses S, Senkel S. Tagging muscle cell lineages in development and tail regeneration using Cre recombinase in transgenic *Xenopus*. Nucleic Acids Res. 2003; 31:e44. [PubMed: 12682379]

Sadaghiani B, Thiébaud CH. Neural crest development in the *Xenopus laevis* embryo, studied by interspecific transplantation and scanning electron microscopy. Dev Biol. 1987; 124:91–110. [PubMed: 3666314]

Schreiber AM, Brown DD. Tadpole skin dies autonomously in response to thyroid hormone at metamorphosis. Proc Natl Acad Sci U S A. 2003; 100:1769–1774. [PubMed: 12560472]

Schreiber AM, Cai L, Brown DD. Remodeling of the intestine during metamorphosis of *Xenopus laevis*. Proc Natl Acad Sci U S A. 2005; 102:3720–3725. [PubMed: 15738398]

Shi, Y-B. Amphibian Metamorphosis. From Morphology to Molecular Biology. Wiley-Liss; New York: 2000.

Smit AL. The ontogenesis of the vertebral column of *Xenopus laevis* (Daudin) with special reference to the segmentation of the metotic region of the skull. Ann Univ Stellenbosch. 1953; 29:79–136.

Smith L. The hyobranchial apparatus of *Spelerpes bislineatus*. J Morphol. 1920; 33:526–583.

Thermes V, Grabher C, Ristoratore F, et al. I-SceI meganuclease mediates highly efficient transgenesis in fish. Mech Dev. 2002; 118:91–98. [PubMed: 12351173]

Thompson, DaR. A quantitative analysis of the cellular and matrix changes in Meckel's cartilage in *Xenopus laevis*. J Anat. 1987; 151:249–254. [PubMed: 3654355]

Toerien M. Experimental studies on the origin of the cartilage of the auditory capsule and columella in *Ambystoma*. J Embryol Exp Morphol. 1963; 11:459–473. [PubMed: 14061953]

Trueb L, Hanken J. Skeletal development in *Xenopus laevis* (Anura: Pipidae). J Morphol. 1992; 214:1–41. [PubMed: 1433306]

Wassersug RJ, Hoff K. Developmental changes in the orientation of anuran jaw suspension. Biol J Linn Soc. 1979; 12:225–259.

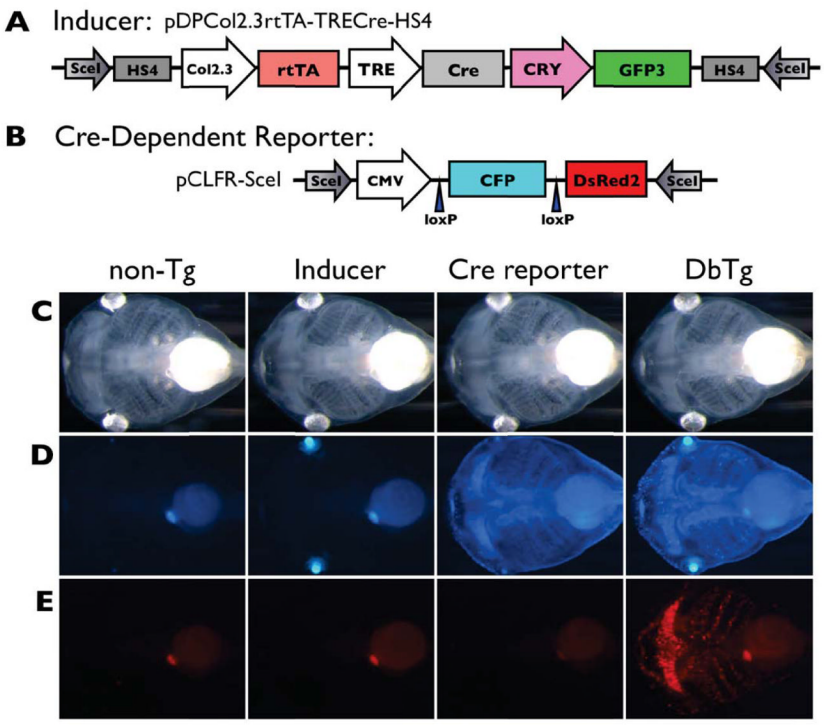

Figure 1.

The Cre-dependent cartilage labeling system. **A, B)** This system uses an inducer transgenic line (pDPCol2.3rtTA-TRECre-HS4) that expresses Cre recombinase in cartilages to act on loxP sites in a Cre-reporter transgene in a second line (pCLFR-SceI)—resulting in DsRed2 replacing CFP in chondrocytes, thereby establishing DsRed2 expression in cartilage under control of the constitutive CMV promoter. The inducer line was designed for doxycycline (Dox) activation of Cre expression through the rtTA/TRE (TetOn) system. However, as shown in the next panel, *col2a1* regulatory elements drive both rtTA and Cre expression, bypassing the TRE promoter and Dox control resulting in loss of inducible control. **C, D, E)** Inducer and Cre-reporter transgenic lines were crossed and two week-old tadpoles not treated with Dox are shown in bright field (**C**), blue (**D**), and red (**E**) fluorescent images. Double transgenics have both the inducer, revealed by GFP (green fluorescent protein) expression in the eyes driven by the lens-specific gamma crystallin (CRY) promoter, and the reporter, revealed by ubiquitous CFP (cyan fluorescent protein) driven by the CMV (cytomegalovirus) promoter. The four expected types of progeny were identified: 1) non-transgenic, 2) pCLFR-SceI single transgenics (CFP in the bodies), 3) pDPcol2.3rtTA-TRECre-HS4 single transgenics (GFP in the eyes, seen as a blue-green color in the blue images), and 4) double transgenics (GFP in the eyes and CFP in the body). Note that in the absence of Dox, DsRed2 fluorescence is visible in larval cartilages in double transgenic animals (**E,** right corner - see text for explanation).

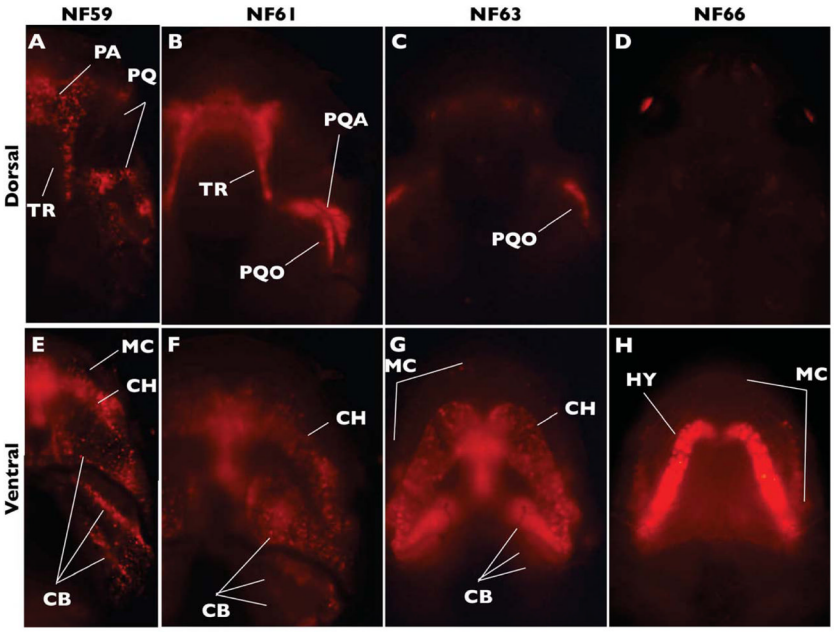

Figure 2.

The Cre-dependent system labels early forming larval cartilages with DsRed2 under the short-lived CMV promoter in double transgenic tadpoles. Images show dorsal and ventral views of DsRed2-labeled cartilage at the indicated NF stages. Note highest intensity of signal in the remodeling palatoquadrate (PQ) and cranial trabeculae (TR; **A–C**), and eventual loss of signal in all dorsal cartilages (**D**). Also note Meckel's cartilage (MC) and ceratohyal (CH) persist in modified form through NF66 (**E–H**). No expression was detected in either the nasal capsule cartilages or otic capsules (see text for explanations.) Additional abbreviations: CB, ceratobranchial; HY, hyale; PA, planum antorbital; PQA, ascending process of the palatoquadrate; PQO, otic process of the palatoquadrate.

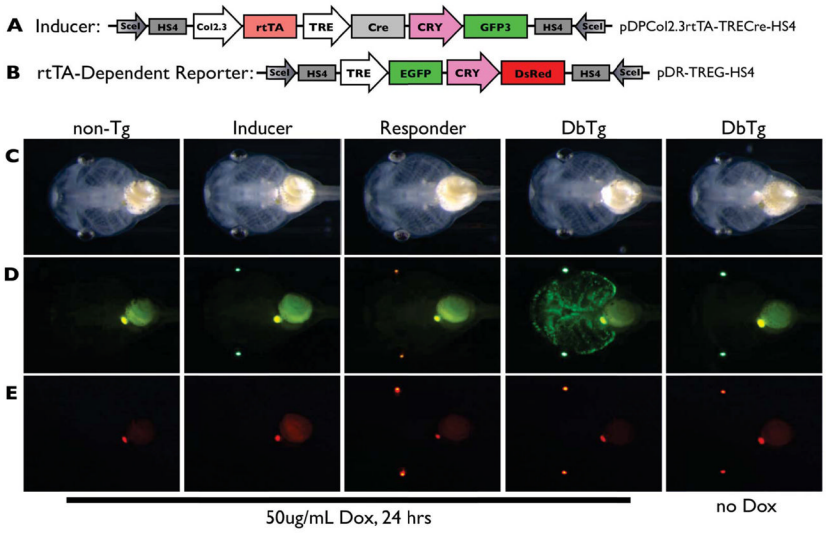

Figure 3.

The rtTA-dependent cartilage labeling system. **A, B)** This system labels cartilage using the same transgenic inducer line as the Cre-dependent system and a reporter line with Dox-inducible GFP expression under control of the TRE promoter. The longevity of inducible GFP protein in newly formed cartilage is used to label and track chondrocytes. The reporter construct allows Dox-inducible expression of GFP wherever rtTA from the inducer line is expressed (i.e., chondrocytes). **C–E)** Inducer and GFP reporter transgenic lines were crossed and two week old tadpoles were treated with or without 50μg/mL Dox for 24 hrs. Bright field (**C**) and green (**D**) and red (**E**) fluorescent images are shown. The four expected types of progeny were identified by examining fluorescent protein expression in the eyes (GFP for the inducer and DsRed2 for the reporter). Note that cartilage-specific GFP expression is evident only in double transgenic tadpoles treated with Dox.

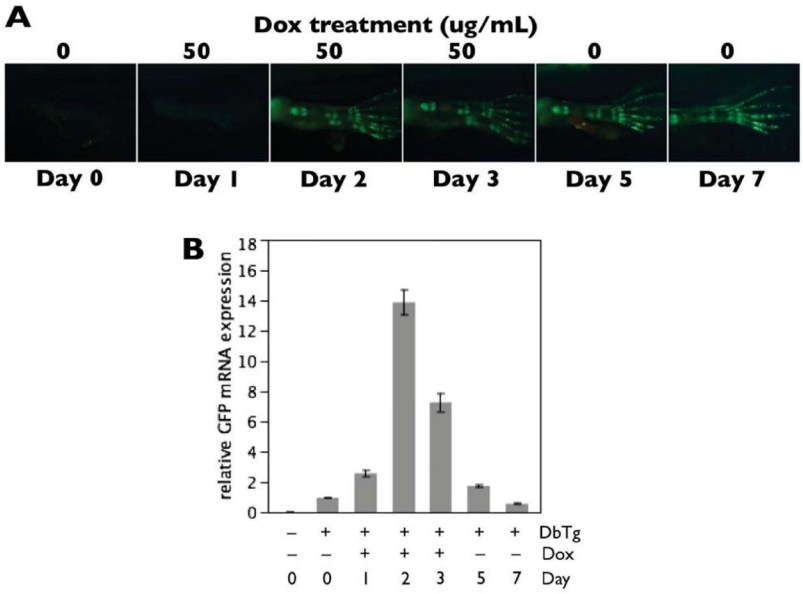

Figure 4.

GFP mRNA and protein stability in transgenic animals from the rtTA-dependent system. **A)** Double transgenic tadpoles were treated with 50μg/mL Dox for 3 days at NF57. Green fluorescence images of the hind limbs were taken on Days 0–3, 5 and 7. GFP protein became strongly visible starting on Day 2 and remained intense through Day 7—four days after Dox removal. **B)** GFP mRNA was measured using quantitative real-time PCR from hind limbs corresponding to the images in the previous panel, n = 3 pairs of limbs per day. Minimal GFP mRNA was detectable in transgenic animals in the absence of Dox, and GFP mRNA expression reached a peak at 2–3 days of Dox treatment. By 2–4 days after Dox removal, GFP mRNA quickly returned to pre-Dox levels. Note that the persistence of inducible GFP protein expression, after GFP mRNA has degraded, renders this system useful for labeling and tracking tadpole cartilages through metamorphosis.

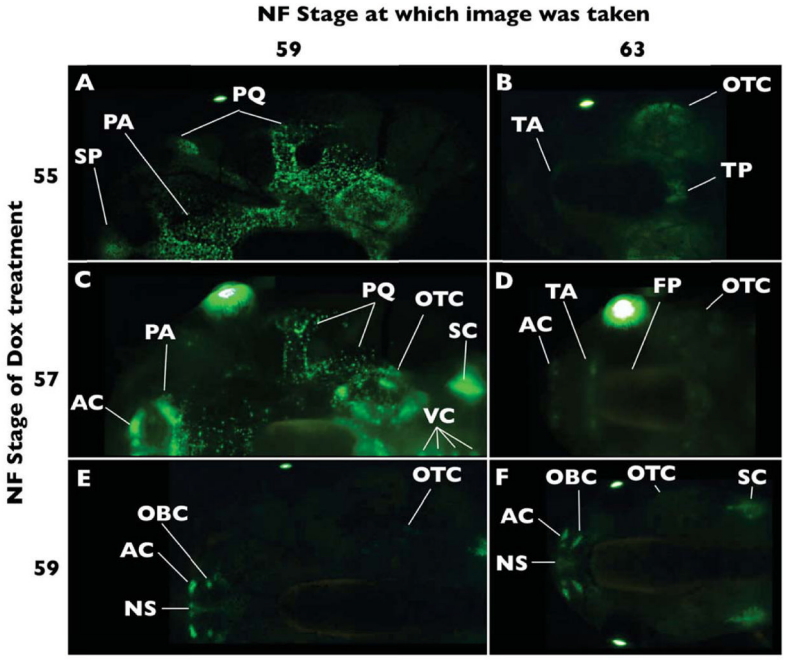

Figure 5.

Tracing dorsal cranial cartilages labeled with GFP in the rtTA-dependent system. Double transgenic tadpoles were treated with Dox at the indicated stages and then imaged at the indicated stages. **A)** Dox-induction at NF55 labels larval cartilage elements. **B)** By NF63, only the otic capsules (OTC) and tectum posterius (TP) carry strong GFP protein expression. Faint expression is also found in the tectum anterius (TA). **C)** Dox-induction at NF57 still labels most larval cartilages, though at lower intensity compared to Dox-induction at NF55. In addition, GFP labeling becomes evident in precursors of the adult alary cartilages (AC). **D)** Alary, tecti anterius and posterius, and otic capsule labeling is retained. Faint expression also surrounds the braincase, corresponding to the area covered by the frontoparietal bone (FP). **E)** Dox-induction at NF59 fails to label larval cartilages, except weak expression in the otic capsule, which persists to NF63. The nasal capsule cartilages are strongly labeled and **F)** remain so through NF63. Additional abbreviations: NS-nasal septum, OBC-oblique cartilage, PA-planum antorbitale, PQ-palatoquadrate, Sc-scapula, SP-suprarostral plate, VC-vertebral column.

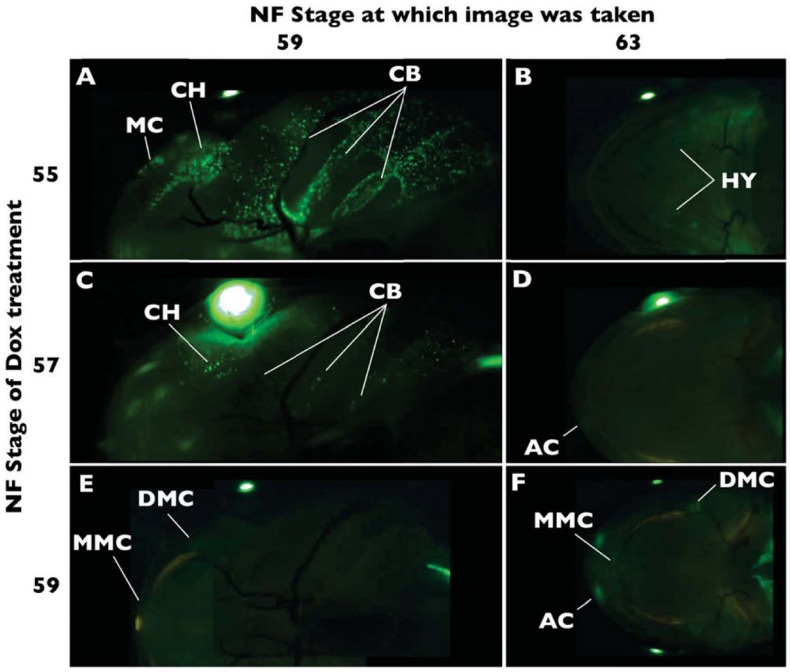

Figure 6.

Tracing ventral cranial cartilages labeled with GFP using the rtTA-dependent system. **A)** Dox-induction at NF55 labels larval cartilage elements, while **B)** only the hyale (HY) is detectable by NF63. **C)** Dox-induction at NF57 still labels all larval cartilage, though at lower intensity compared to Dox-induction at NF55. **D)** GFP labeling in the hyale is not detectable at NF63 following later induction, but is apparent in the adult alary cartilages (AC; see Figure 5). **E)** Dox-induction at NF59 has barely detectable GFP-labeling in distal (DMC) and medial (MMC) ends Meckels's cartilage. **F)** By NF63, distal (DMC) and medial (MMC) ends Meckels's cartilage are still labeled but in their remodeled position. Portions of the nasal capsule from the dorsal side show though at NF63. Additional abbreviations: CB-ceratobranchial, CH-ceratohyal, MC-Meckel's cartilage.

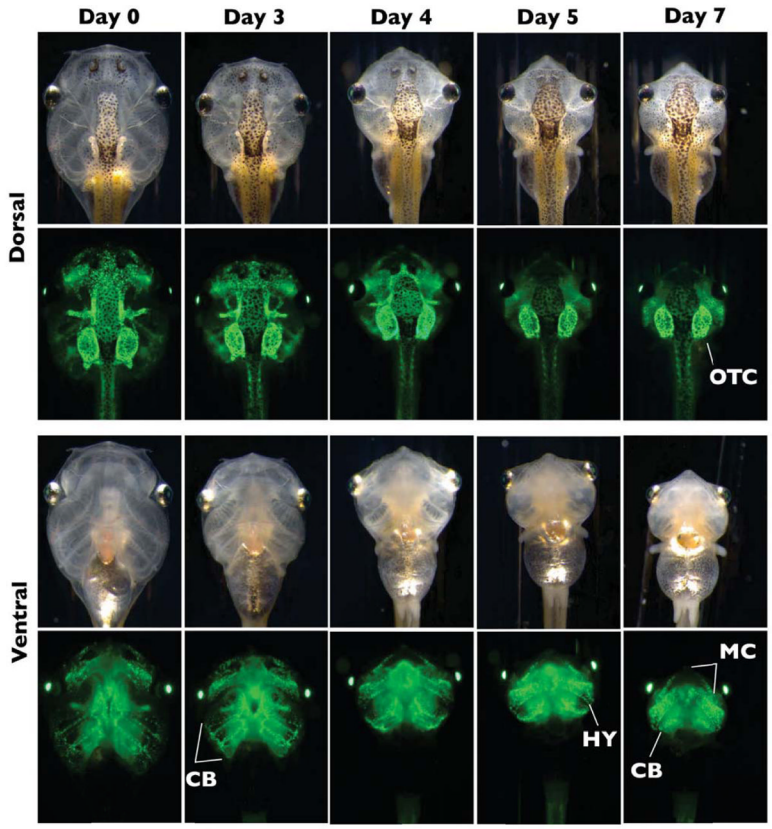

Figure 7.

Tracing cranial cartilages through T3-induced metamorphosis using the rtTA-dependent system. One-week-old double transgenic tadpoles were treated with 50μg/mL Dox for 2 days then treated with 10nM T3 for 7 days in the absence of Dox. Brightfield and green fluorescence dorsal and ventral images were taken on Days 0, 3, 4, 5, and 7 of T3 treatment. All larval cartilages were well-labeled by the beginning of the T3 treatment. Note that the otic capsule (OTC) is the only labeled cartilage remaining in dorsal view, while the remodeling hyale (HY), elongating Meckel's cartilage (MC), and degenerating ceratobranchials (CB) are visible in the ventral view.

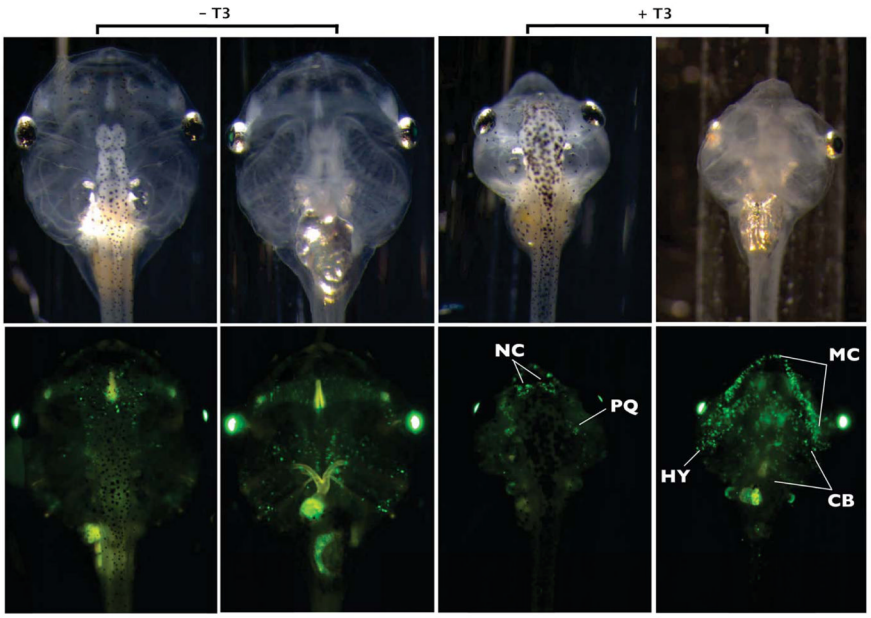

Figure 8.

Tracing cranial cartilages after initiation of T3 treatment in early tadpoles using the rtTA-dependent system. One week old double transgenic tadpoles were treated with 10nM T3 for three days then treated with 10nM T3 and 50μg/mL Dox for the next four days. Sibling double transgenic tadpoles treated with Dox and not T3 served as controls. No food was given during T3 treatment in treated or control tadpoles. Brightfield and green fluorescence dorsal and ventral images were taken on Day 7 of T3 treatment. Compared to Fig. 7, GFP labeling intensity in the non-T3-treated controls was much reduced, likely due to starvation and lack of new cartilage formation. In the T3-treated tadpoles, newly formed cartilage is marked, representing nasal capsule cartilages (NC), elongating Meckel's cartilage (MC), and remodeling hyale (HY). Punctate expression also occurs on the largely resorbed palatoquadrate (PQ) and ceratobranchials (CB).

Table 1

Summary of experimental support for cartilages at NF63 and NF66 that are derived from larval chondrocytes. NA - no available evidence from the experiment.

Cartilage element	Cre-dependent system	rtTA-dependent system	Induced metamorphosis
Tectum posterius	NA	+	NA
Tectum anterius	NA	+	NA
Otic capsule	NA	+	+
Meckel's cartilage	+	NA	+
Hyale	+	+	+